Reconstruction of 3D Radial MRI with Linogram Sampling

Naoharu Kobayashi[1], Djaudat Idiyatullin[1], Curtis A Corum[1], and Michael Garwood[1]

[1]*Center for Magnetic Resonance Research, University of Minnesota, Minneapolis, Minnesota, United States*

Introduction

In radial MRI, k-space is sampled in a radial manner, namely, on a polar coordinate system. Reconstruction of radial MRI is typically performed with gridding or filtered backprojection. In gridding reconstruction, the acquired data is resampled to a Cartesian k-space by convolving with an interpolation kernel and then performing Fourier transformation (FT). In filtered backprojection, FT is performed in polar coordinates, and resampling from polar to Cartesian coordinates is performed along with the integration over angular variables. For both methods, the resampling and sampling density correction correspond to interpolation and calculation of the Jacobian in the Fourier integral, respectively. Linogram sampling, introduced to radial MRI about 20 years ago, is a "semi-Cartesian" k-space sampling method, where the sampling pattern is a concentric square (2D)[1] or cubic grid (3D)[2] as shown in Fig.1a. For linogram sampling, there is a corresponding reconstruction algorithm known as linogram reconstruction that does not need explicit interpolation and simplifies the Jacobian calculation, i.e. density correction. Therefore, linogram reconstruction may improve resolution, minimize interpolation errors, and reduce computational time. In this study, we show point spread functions (PSF) and reconstructed images from 3D linogram data that were calculated with the three reconstruction methods: gridding, backprojection and linogram reconstruction. The linogram data were obtained in two separate ways: a Bloch simulation and an experiment with SWeep Imaging with Fourier Transformation (SWIFT)[3].

Method

3D simulation data were generated by numerically integrating the Bloch equation. Sequence parameters in the numerical SWIFT simulation were as follow: bandwidth = 125 kHz, flip angle = 10°, hyperbolic secant (HS1) gapped pulse excitation, $T_2^* = 20$ ms, # of sampling points = 256, and # of views = 46,464. A 3D theoretical phantom shown in Fig.3a was used for the simulation. A SWIFT experiment was performed in a 9.4T 31 cm horizontal bore magnet with parameters comparable to the numerical simulation, with the exception of: nominal flip angle = 6°, TR = 2.3 ms, and FOV=7.0x7.0x7.0 cm^3. Measurement was done on a 50 mM $MnCl_2$ phantom that was fixed with 1.5% agar and that held a spouted cylindrical Teflon object inside.

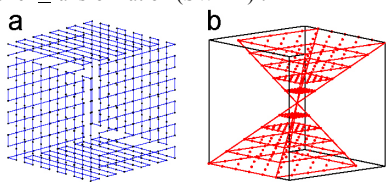

Figure 1. (a) 3D linogram sampling pattern. (b) One of the three orthogonal double pyramids for linogram reconstruction.

Calculation of PSFs and image reconstruction were performed with in-house developed C code. The reconstruction programs were parallelized with openMP[4] for gridding and linogram reconstruction and MPI[5] for backprojection. All the programs were run using an Intel Quad-Core Xenon X5470 3.33 GHz processor.

Gridding was performed according to the previous report[6]. Kaiser-Bessel window function with 3 pixel width in data space and 2 times oversampling were used. Sampling density correction was performed in an iterative manner[7] (3 times iteration). After gridding, we applied FT and got a 3D image.

In backprojection, the Fourier integral is expressed by using the second derivative of the projection $P(r,\phi,\theta)$[8] as

$$\rho(x,y,z) = -\frac{1}{8\pi^3}\int_0^{2\pi}\int_0^{\pi} W(\phi,\theta)\cdot\frac{\partial^2 P(r,\phi,\theta)}{\partial r^2}\,d\phi d\theta,$$

where $\rho(x,y,z)$ is the image to be reconstructed and $W(\phi,\theta)$ is a weighting function that is an angular component of the Jacobian, i.e., an angular density correction factor. In linogram sampling, $W(\phi,\theta)=(\mathbf{n}\cdot\mathbf{g})^2$, in which $\mathbf{n}$ is a unit vector that is normal to the plane of the sampling cube and $\mathbf{g}=(\sin\theta\cos\phi, \sin\theta\sin\phi, \cos\theta)$ that orients to the applied gradient direction.

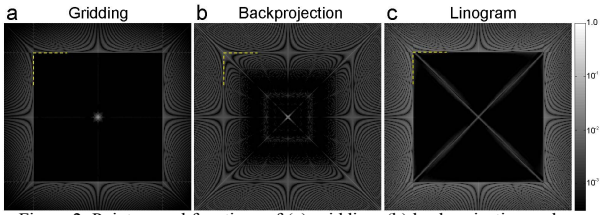

Figure 2. Point spread functions of (a) gridding, (b) backprojection and (c) linogram reconstruction for linogram sampling data.

In linogram reconstruction, the linogram k-space was divided into three non-overlapping mutually orthogonal double pyramids (Fig.1b). Each of them was composed of planes on which data points were rectilinear and equispaced. Each plane had different spacing between the data points and thus the general discrete FT does not work. Therefore, we applied 2D FT to each plane separately using chirp-Z transform[9], which performs simultaneous 2D scaling and FT. We applied general 1D FT along the remaining dimension that is perpendicular to the 2D chirp-Z planes and then summed up the three data sets to get a 3D image.

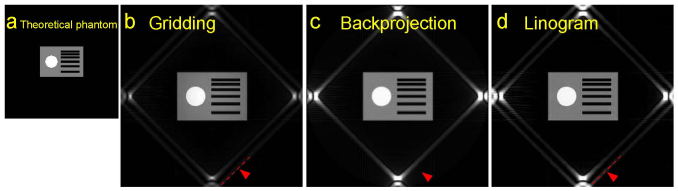

Figure 3. A simulated theoretical phantom (a) and reconstructed images from gridding (b), backpronection (c), and linogram reconstruction (d).

Results and Discussion

PSFs from the three reconstruction methods are shown in Fig.2. PSFs from gridding and linogram reconstruction showed a sharp edge due to aliasing (yellow dashed lines in Fig.2a,c), which was not observed in the PSF from backprojection (Fig.2b), because FT was calculated in polar coordinates for backprojection.

Images from the Bloch simulation of SWIFT are shown in Fig.3. All three methods provided similar images, but the image from backprojection had slightly more blurring due to direct interpolation in image space (i.e., linear interpolation was used in backprojection) or possibly the choice of filtering. Using more appropriate interpolation methods such as cubic convolution interpolation and Lanczos interpolation may improve the image resolution. The difference in aliasing effects between backprojection and the other two methods is also apparent in the reconstructed images. In the images from gridding and linogram reconstruction, there were double rhombic lines, the outer of which should be aliasing signals from the inner one (red dashed lines in Fig.3b,d). However, there was a single line found in the image from backprojection. Images from a SWIFT experiment showed the same trend as the numerical simulation (Fig.4).

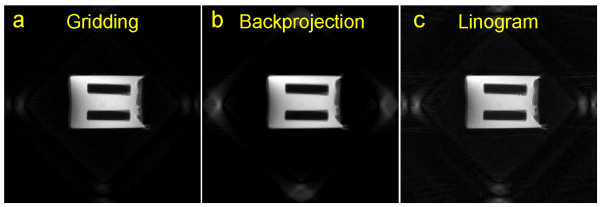

Figure 4. Images reconstructed from phantom experiment data with gridding (a), backprojection (b) and linogram reconstrucion(c)

One big difference between the three methods is the computational cost. Computational time for reconstruction is 83 s, 1297 s, and 27 s for gridding, backprojection and linogram reconstruction, respectively. In gridding, the majority of the time is spent for calculation of the density correction, whereas it is very simple for linogram reconstruction, since the Jacobian in the 2D Fourier integral is constant on each rectilinear and equispaced plane. While the computational time for gridding and backprojection is proportional to the total number of views, linogram reconstruction is relatively independent of the view number. Accordingly, linogram reconstruction is advantageous for reconstruction of high resolution (large number of views) data.

Acknowledgements

This research is supported by National Institutes of Health grant P41 RR008079 and R21 CA139688, and WM KECK Foundation.

References

(1) Axel L. et.al., *IEEE Trans. Med. Imag.* 9:447-449, 1990. (2) Herman GT. et.al., *Phys. Med. Biol.* 37:673-687, 1992. (3) Idiyatullin D. et.al., *JMR* 181:342-349, 2006. (4) http://openmp.org (5) http://www.mcs.anl.gov/research/projects/mpich2 (6) Jackson JI. et.al., *IEEE Trans. Med. Imag.* 10:473-478, 1991. (7) Pipe J.G, et.al., *MRM* 41:179-186, 1999. (8) Wu C. et.al., *Lecture Notes in Comput. Sci.* 687:387-400, 1993. (9) Rabiner LR., et.al., *IEEE Trans. Audio Electroacoust.* AU-17:86-92, 1969.